Published online: December 5, 2016

Article

TRANSPARENT PROCESS

EMBO reports

Mitochondrial–nuclear co-evolution leads to hybrid incompatibility through pentatricopeptide repeat proteins

Han-Ying Jhuang[1,2], Hsin-Yi Lee[1,3] & Jun-Yi Leu[1,2,*]

Abstract

Mitochondrial–nuclear incompatibility has a major role in reproductive isolation between species. However, the underlying mechanism and driving force of mitochondrial–nuclear incompatibility remain elusive. Here, we report a pentatricopeptide repeat-containing (PPR) protein, Ccm1, and its interacting partner, 15S rRNA, to be involved in hybrid incompatibility between two yeast species, *Saccharomyces cerevisiae* and *Saccharomyces bayanus*. *S. bayanus*-Ccm1 has reduced binding affinity for *S. cerevisiae*-15S rRNA, leading to respiratory defects in hybrid cells. This incompatibility can be rescued by single mutations on several individual PPR motifs, demonstrating the highly evolvable nature of PPR proteins. When we examined other PPR proteins in the closely related *Saccharomyces sensu stricto* yeasts, about two-thirds of them showed detectable incompatibility. Our results suggest that fast co-evolution between flexible PPR proteins and their mitochondrial RNA substrates may be a common driving force in the development of mitochondrial–nuclear hybrid incompatibility.

Keywords hybrid incompatibility; mitochondrial–nuclear co-evolution; PPR protein; yeast speciation

Subject Category Evolution

DOI 10.15252/embr.201643311 | Received 7 September 2016 | Revised 9 October 2016 | Accepted 21 October 2016 | Published online 5 December 2016

EMBO Reports (2017) 18: 87–101

Introduction

A critical step of speciation is the emergence of reproductive isolating barriers between diverging populations. These barriers are classified into two major forms: (i) prezygotic isolation caused by mating discrimination or unsuccessful gamete recognition, and (ii) postzygotic isolation caused by hybrid inviability or sterility. Identifying the molecular mechanisms underlying reproductive isolation would allow us to deduce the driving force of speciation. Yeasts have proven to be an excellent model organism for studying postzygotic isolation, helping to demonstrate the involvement of anti-recombination induced by DNA sequence divergence, chromosomal rearrangements, and genetic incompatibility [1–5]. Apart from DNA sequence divergence, which can occur simply by mutation accumulation, development of postzygotic isolation is often deemed a by-product of adaptive selection [6]. In the classical genetic incompatibility model, environmental adaptation is hypothesized to be an important force driving fixation of diverging alleles in different populations [7]. However, many known instances of genetic incompatibility seem to be caused by susceptibility to mutation pressure and invasion of pathogens or selfish genetic elements [8]. Fixation of divergent alleles involved in incompatibility can be achieved by repeated mutation compensation processes or during the resolution of genetic conflicts [9,10]. Drawing a general picture of how genetic incompatibility evolved entails identification of more incompatibility genes.

Mitochondrial–nuclear incompatibility is a specific form of Dobzhansky–Muller incompatibility [11–13]. Mitochondria play essential roles in the survival, growth, and sexual reproduction of organisms [14]. During evolution, selective pressures for better maintenance or enhanced fixation of beneficial mutations in mitochondrial genes have led to transfer of most mitochondrial genes to the nuclear genome, leaving only a handful of protein-coding genes in modern mitochondrial genomes (mtDNA) [15–18]. In the budding yeast *S. cerevisiae*, there are around 1,000 nucleus-encoded mitochondrial proteins, whereas the mtDNA encodes only eight proteins [19]. Compared to the nuclear genome, the mutation rate of mtDNA is generally an order of magnitude higher [20]. To maintain proper interactions, nucleus-encoded mitochondrial proteins may need to rapidly co-evolve with mtDNA [21–23]. Consequently, mismatched mitochondrial and nuclear genomes have been observed to cause inter- or intraspecific hybrid incompatibilities in a broad range of species, even though the molecular basis of incompatibility was not identified in most cases [12,24–32].

Among the closely related *Saccharomyces sensu stricto* yeast species, several genes involved in mitochondrial–nuclear hybrid incompatibility have been characterized at the molecular level.

1 Graduate Institute of Life Sciences, National Defense Medical Center, Taipei, Taiwan
2 Institute of Molecular Biology, Academia Sinica, Taipei, Taiwan
3 Molecular and Cell Biology, Taiwan International Graduate Program, Graduate Institute of Life Sciences, National Defense Medical Center and Academia Sinica, Taipei, Taiwan
*Corresponding author. Tel: +886 2 26519574; E-mail: jleu@imb.sinica.edu.tw

Nucleus-encoded Mrs1 regulates intron removal of the mitochondrion-encoded *COX1* mRNA [33–35]. Mrs1 splices two of the *S. paradoxus COX1* introns, but one of these introns was lost in *S. cerevisiae* during evolution. *S. cerevisiae* Mrs1 fails to splice both introns of the *S. paradoxus COX1* gene in hybrid cells, resulting in hybrid incompatibility between *S. cerevisiae* and *S. paradoxus* [36]. Nucleus-encoded Aim22 is an enzyme required for lipoylation of mitochondrial targets [37–39]. *S. cerevisiae* Aim22 cannot function properly in an *S. bayanus* mitochondrial genomic background, though the incompatible interacting partners remain elusive [36]. Similarly, Aep2 is a nucleus-encoded pentatricopeptide repeat (PPR) protein required for translation of *OLI1* mRNA, which encodes for F_0-ATP synthase subunit c [40,41]. *S. bayanus* Aep2 is incompatible with the *S. cerevisiae OLI1* gene, so synthesis of the Oli1 protein is inhibited [29]. Despite that the incompatibility of both Mrs1 and Aep2 involve protein–RNA interactions, it is necessary to identify more genes in order to elucidate whether this is a common mode of mitochondrial–nuclear incompatibility.

Pentatricopeptide repeat proteins are often observed to regulate mitochondrial RNA and these proteins constitute one of the largest protein families in eukaryotes, mainly contributed by expanded plant PPR genes [42]. The pentatricopeptide repeat is a degenerate 35-amino acid structural motif, and multiple tandem PPR motifs in the PPR protein act in a coordinated modular manner, which might allow PPR proteins to evolve rapidly [43–45]. In land plants, expansion of the PPR family has been speculated to have had important impacts on the evolution of organellar genome complexity [46]. The *S. cerevisiae* genome contains 15 predicted PPR genes [41,47]. Deletion of PPR genes often leads to decreased respiratory growth in yeast [47,48]. Although these proteins have been shown to evolve more rapidly than the entire genome background in general, their evolutionary trajectories in closely related species have not been characterized [41].

In the present study, we employed a chromosomal replacement strategy to identify another PPR gene, *CCM1*, involved in hybrid incompatibility between *S. cerevisiae* and *S. bayanus*. This incompatibility was bidirectional and could be rescued by a variety of mutations in the PPR motifs. Subsequent systematic replacements of all yeast PPR genes with orthologs from closely related species revealed that PPR genes prevalently contribute to hybrid incompatibility among the *Saccharomyces sensu stricto* yeasts. Our results demonstrate that evolution of mitochondrial–nuclear incompatibility is prevalent in yeast species and PPR proteins play a large role in fast co-evolution of the two genomes.

Results

Chromosome 7 of *Saccharomyces bayanus* is incompatible with the *Saccharomyces cerevisiae* genome

To identify genetic incompatibility between the two closely related yeast species, *S. bayanus* and *S. cerevisiae*, we previously constructed chromosome replacement lines in which one or two chromosomes were derived from *S. bayanus*, and the remaining chromosomes and mtDNA were from *S. cerevisiae* [29]. When all the chromosome replacement lines were examined, we noticed that the replacement line carrying *S. bayanus* chromosome 7 (Sc + Sb-chr7) exhibited obvious defects in both vegetative growth and sporulation, suggestive of defects in mitochondrial respiration. To address that we grew cells in medium containing only the nonfermentable carbon source (i.e., glycerol in the following experiments). The Sc + Sb-chr7 strain showed much reduced growth on glycerol-containing plates, indicating that the mitochondrial function of Sc + Sb-chr7 was compromised (Fig 1A). However, if we crossed Sc + Sb-chr7 with a *S. cerevisiae* haploid strain without mtDNA (Sc-ρ^0), the growth defect was fully rescued, suggesting that the mtDNA of Sc + Sb-chr7 is intact and the observed respiratory defect is recessive (Fig 1A).

The respiratory defect of Sc + Sb-chr7 might result from incompatibility between *S. bayanus* chromosome 7 and other *S. cerevisiae* chromosomes or mtDNA. To address this issue, we generated two hybrid diploids: In the first one (Sc + Sb-chr7 × Sb-ρ^0), a whole set of *S. bayanus* chromosomes were provided but mtDNA was from *S. cerevisiae*, and in the second hybrid (Sc + Sb-chr7-ρ^0 × Sb), it contained both *S. bayanus* chromosomes and mtDNA. The chr 7 incompatibility was fully rescued in the second hybrid, but only partially rescued in the first one (Fig 1A). These results indicate that the incompatibility is mainly between *S. bayanus* chromosome 7 and *S. cerevisiae* mtDNA (Sc-mtDNA), and the interactions between different chromosomes only contribute minor effects.

CCM1 is involved in the incompatibility between *Saccharomyces bayanus* chromosome 7 and the *Saccharomyces cerevisiae* mitochondrial genome

We performed a genomic DNA library screen to search for *S. cerevisiae* gene(s) that could rescue the growth defect of Sc + Sb-chr7 on glycerol plates. Two different clones were obtained from the screen and both of them contained the full-length *S. cerevisiae CCM1* gene (*Sc-CCM1*), which is also located on chromosome 7. To verify the involvement of *CCM1* in hybrid incompatibility, we PCR-amplified the *CCM1* gene from *S. cerevisiae* genomic DNA, cloned it into a single-copy plasmid, and tested its ability to rescue the growth defect of Sc + Sb-chr7. Expression of *Sc-CCM1* in Sc + Sb-chr7 exhibited a considerable rescue effect (Fig 1B). We also constructed allele replacement strains in which the native *CCM1* ORF in *S. cerevisiae* was replaced by the *S. bayanus CCM1* orthologous allele and a nutrient marker (*HIS3*) or simply placed the nutrient marker in the downstream of *CCM1* as a control (Sc + *Sb-CCM1* and Sc + *Sc-CCM1*, respectively). Only the Sc + *Sb-CCM1* strain showed substantial growth defects on glycerol plates, suggesting that the Sb-Ccm1 protein is incompatible with the *S. cerevisiae* genetic background (Fig 1C).

In *S. cerevisiae*, *CCM1* encodes a mitochondrial protein essential for pre-mRNA intron removal of two mtDNA-encoded genes, *COX1* and *COB* [49]. In addition, the Ccm1 protein directly interacts and stabilizes mitochondrial 15S rRNA [50]. Therefore, *CCM1* incompatibility is likely related to its functions in the mitochondria. We tested this idea by crossing the Sc + *Sb-CCM1* strain to *S. bayanus* with or without mtDNA. *Sb-CCM1* incompatibility could only be rescued in the presence of the *S. bayanus* mtDNA (Sc + *Sb-CCM1*-ρ^0 × Sb), indicating that *Sb-CCM1* is incompatible with Sc-mtDNA (Fig 1C).

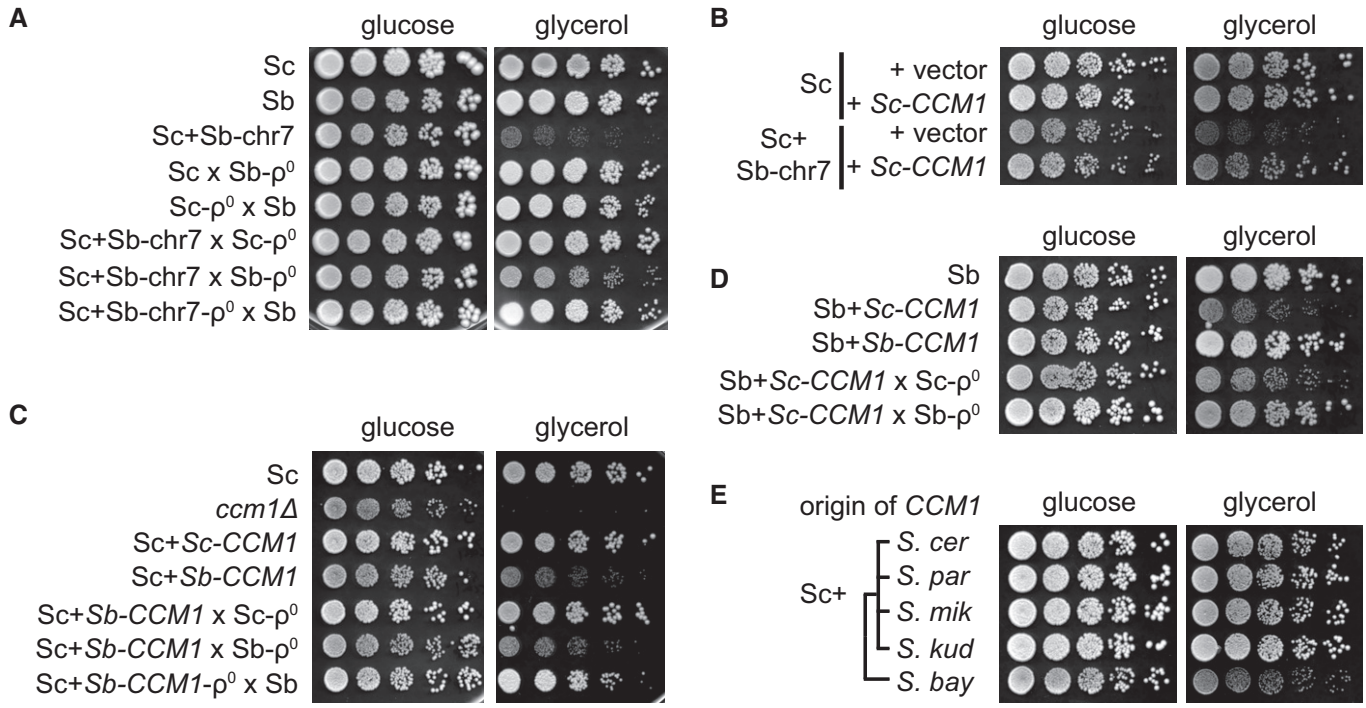

Figure 1. *CCM1* is involved in the incompatibility between *S. bayanus* chromosome 7 and the *S. cerevisiae* mitochondrial genome.

A Chromosome 7 of *S. bayanus* is incompatible with the *S. cerevisiae* genome. The chromosome 7 replacement stain (Sc + Sb-chr7) exhibited serious growth defects when grown on the nonfermentable carbon source (glycerol). The respiration defects could be partially rescued when a whole set of *S. bayanus* chromosomes were provided (Sc + Sb-chr7 × Sb-ρ^0), or fully rescued with the addition of *S. bayanus* mtDNA (Sc + Sb-chr7-ρ^0 × Sb). Cell cultures were serially diluted and spotted onto YPD (glucose) or YPG (glycerol) plates. The plates were then incubated at 28°C until colonies were easily observed.

B Ectopically expressing *Sc-CCM1* rescues the respiration defect of Sc + Sb-chr7. Spot assays for the wild-type *S. cerevisiae* (Sc) and the chromosome 7 replacement stain (Sc + Sb-chr7) carrying an empty plasmid (+ vector) or the plasmid with the *S. cerevisiae CCM1* gene (*+ Sc-CCM1*).

C *Sb-CCM1* incompatibility could only be rescued in the presence of *S. bayanus* mtDNA. The native *CCM1* ORF in *S. cerevisiae* was replaced by either *Sb-CCM1* (Sc + *Sb-CCM1*) or *Sc-CCM1* (Sc + *Sc-CCM1*, as a control) coding regions. Crossing the Sc + *Sb-CCM1* strain with the mtDNA-less Sb-ρ^0 strain (Sc + *Sb-CCM1* × Sb-ρ^0) could not rescue the growth defect.

D *CCM1* incompatibility is symmetric between *S. cerevisiae* and *S. bayanus*. The *CCM1* ORF in *S. bayanus* was replaced by either *Sc-CCM1* (Sb + *Sc-CCM1*) or *Sb-CCM1* (Sb + *Sb-CCM1*, as a control) coding regions. Only the Sb + *Sc-CCM1* strain exhibited respiration defects and the defect could not be rescued even when a whole set of *S. cerevisiae* chromosomes were provided (Sb + *Sc-CCM1* × Sc-ρ^0).

E *CCM1* incompatibility probably occurred during the divergence between *S. bayanus* and the common ancestor of *S. cerevisiae*, *S. paradoxus*, *S. mikatae*, and *S. kudriavzevii*. The endogenous *CCM1* in *S. cerevisiae* was replaced with its orthologous alleles from other *Saccharomyces sensu stricto* yeasts. Only the strain carrying *S. bayanus CCM1* displayed growth defects on glycerol-containing plates.

Data information: Sc, *S. cerevisiae*. Sb, *S. bayanus*. ρ^0, mtDNA-less strains.

CCM1 incompatibility is symmetric between *Saccharomyces cerevisiae* and *Saccharomyces bayanus*

Hybrid incompatibility caused by two interacting genetic loci may be unidirectional (asymmetric) if one of the loci remains the ancestral form in parental populations. Alternatively, if both loci have changed, as might be the case of fast-evolving genes, the incompatibility could be bidirectional (symmetric). The mitochondrial–nuclear incompatibilities identified in previous yeast studies are all asymmetric [29,36]. To characterize the symmetry of *CCM1* incompatibility, we replaced the native *CCM1* ORF in *S. bayanus* with the coding region of *Sc-CCM1* and a nutrient marker (*HIS3*), or simply placed the nutrient marker downstream of *Sb-CCM1* as a control (Sb + *Sc-CCM1* or Sb + *Sb-CCM1*, respectively), and examined their fitness. The Sb + *Sc-CCM1* strain exhibited growth defects when cultured on glycerol-containing plates (Fig 1D). Furthermore, the incompatibility could be rescued by crossing Sb + *Sc-CCM1* with the *S. bayanus* ρ^0 strain to supply a whole set of *S. bayanus* chromosomes, but was not rescued when crossed with the *S. cerevisiae* ρ^0 strain (Fig 1D). The results indicate that *CCM1* is involved in a symmetric mito-nuclear incompatibility between *S. cerevisiae* and *S. bayanus*.

Both *S. cerevisiae* and *S. bayanus* belong to the *Saccharomyces sensu stricto* group. To fine-map in which branch *CCM1* incompatibility evolved, we replaced native *CCM1* in *S. cerevisiae* with its orthologous alleles from other *Saccharomyces sensu stricto* yeasts, including *S. paradoxus*, *S. mikatae*, or *S. kudriavzevii*. We found that only the *CCM1* orthologous allele from *S. bayanus* was incompatible with the *S. cerevisiae* genetic background (Fig 1E). These results suggest that *CCM1* incompatibility probably occurred during the divergence between *S. bayanus* and the common ancestor of *S. cerevisiae*, *S. paradoxus*, *S. mikatae*, and *S. kudriavzevii*.

Sb-CCM1 incompatibility leads to reduced levels of mitochondrial 15S rRNA

One possible explanation for the *Sb-CCM1* incompatibility is that the Sb-Ccm1 protein cannot be transported efficiently to Sc-mitochondria. We used subcellular fractionation to determine the localization of Ccm1. Mitochondria from wild-type *S. cerevisiae* strains carrying *Sc-CCM1-13Myc* or *Sb-CCM1-13Myc* were isolated and examined using Western blotting. Although a low level of Sb-Ccm1 was detected in the cytosolic fraction, the majority of Sb-Ccm1 localized to mitochondria, indicating that mislocalization was not the cause of hybrid incompatibility (Fig 2A).

Because Ccm1 affects both pre-mRNA splicing of *COX1* and *COB*, and stability of 15S rRNA [49–51], we used Northern blots to examine whether the steady-state levels or maturation of the transcripts from mtDNA-encoded genes was affected in the Sc + *Sb-CCM1* strain. For all the examined mtDNA-encoded genes, only 15S rRNA showed a reduced level in Sc + *Sb-CCM1* cells (Fig 2B). No differences were detected in the mRNA levels of *COX1* and *COB* between the Sc + *Sb-CCM1* and Sc + *Sc-CCM1* strains. To elucidate the mechanism underlying reduced levels of 15S rRNA, we tested whether the interaction between 15S rRNA and the Sb-Ccm1 protein is impeded in Sc + *Sb-CCM1* cells. We expressed either C-terminally Myc-tagged Sc-Ccm1 or Sb-Ccm1 in *S. cerevisiae* strains, isolated the mitochondria, and then immunoprecipitated Ccm1 via the anti-Myc antibody. The level of Ccm1-bound 15S rRNA was then measured using real-time quantitative PCR, and the mRNAs of a nucleus-encoded gene *TDH3* and a mtDNA-encoded gene *COB* were used as the negative controls (see Materials and Methods). We found that levels of co-immunoprecipitated *S. cerevisiae* 15S rRNA were more enriched in the strains carrying Sc-Ccm1 than those with Sb-Ccm1 (330.0 ± 15.4 vs. 7.1 ± 0.4 fold enrichment relative to controls

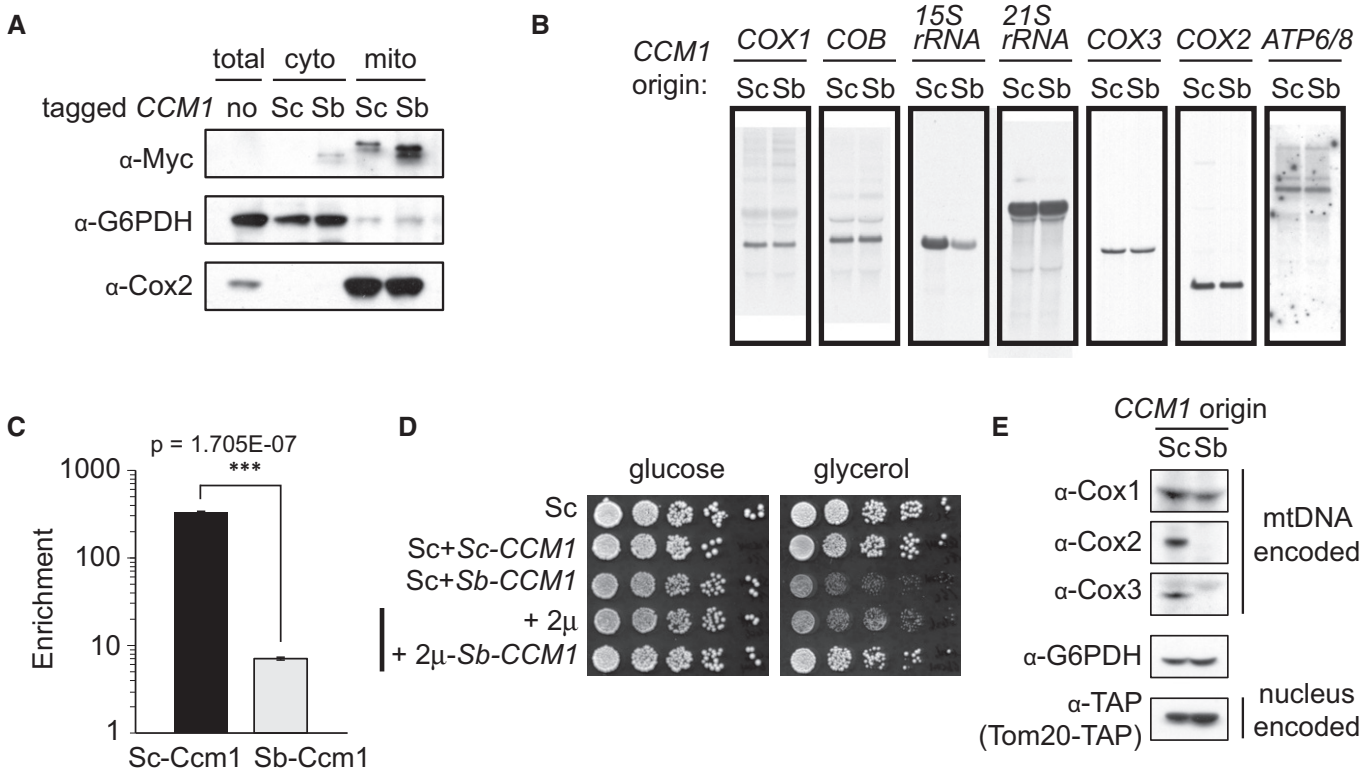

Figure 2. *CCM1* incompatibility results in reduced levels of 15S rRNA and mtDNA-encoded proteins.

A Sb-Ccm1 protein is transported efficiently to *S. cerevisiae* mitochondria. Total cell extracts (total), cytosolic fractions (cyto), or mitochondrial fractions (mito) were hybridized with different antibodies to detect the proteins. G6PDH (glucose-6-phosphate dehydrogenase) and Cox2 served as cytosolic and mitochondrial markers, respectively. Both Sc-Ccm1 and Sb-Ccm1 were fused with c-Myc at the C-terminus and expressed from a single-copy plasmid. The Myc-tagged Ccm1 proteins consistently appeared as double bands, which was probably due to some unknown protein modifications.

B The level of 15S rRNA is reduced in Sc + *Sb-CCM1* cells. RNA isolated from Sc + *Sb-CCM1* (labeled as Sb) or Sc + *Sc-CCM1* (labeled as Sc) cells was hybridized with gene-specific probes using Northern blots.

C Sb-Ccm1 interacts weakly with *S. cerevisiae* 15S rRNA. The level of Ccm1-bound 15S rRNA was measured using quantitative PCR analysis following mitochondrial RNA immunoprecipitation of *S. cerevisiae* cells expressing *Sc-CCM1-13Myc* or *Sb-CCM1-13Myc*. Data were normalized to the control group without the Myc tag to obtain the relative fold enrichment. Graph was plotted using data from three independent repeats for each strain, and *P*-value was calculated by unpaired, two-sided Student's *t*-test. Error bars indicate SD. ***P-value < 0.001.

D Overexpression of *Sb-CCM1* rescues the respiration defect of Sc + *Sb-CCM1* cells. Cell cultures were serially diluted and spotted onto YPD (glucose) or YPG (glycerol) plates. The plates were then incubated at 28°C until colonies were easily observed.

E The steady-state level of mtDNA-encoded proteins is reduced in Sc + *Sb-CCM1* cells. Immunoblotting for the mitochondrial proteins in Sc + *Sb-CCM1* (labeled as Sb) or Sc + *Sc-CCM1* (labeled as Sc) cells. Cox1, Cox2, and Cox3 are mtDNA-encoded complex IV subunits. Tom20 is a nucleus-encoded mitochondrial protein.

without tagging, Fig 2C), while the transcripts of the negative controls were not detected in the elutes. These results suggest that *Sb-CCM1* may function as a hypomorphic mutant of *Sc-CCM1*, and the weakened interaction between Sb-Ccm1 and 15S rRNA might be responsible for the reduced level of 15S rRNA. To further test this weak allele idea, we overexpressed *Sb-CCM1* in *S. cerevisiae* using a 2-micron multi-copy plasmid (pRS426). Indeed, the respiratory defect of Sc + *Sb-CCM1* cells was largely rescued by overexpression of *Sb-CCM1* (Fig 2D).

15S rRNA is an essential component of mitochondrial ribosomes. The decrease in 15S rRNA is likely to cause a reduction in translation of mitochondrion-encoded proteins. We used Western blots to examine Cox1, Cox2, and Cox3, that is, the subunits of mitochondrial complex IV (cytochrome c oxidase) that are encoded on the mtDNA. The steady-state protein levels of Cox1, Cox2, and Cox3 were all reduced in the Sc + *Sb-CCM1* strain (Fig 2E). In contrast, the nucleus-encoded mitochondrial protein, Tom20, was maintained at similar levels in the Sc + *Sb-CCM1* and Sc + *Sc-CCM1* strains.

Experimental evolution to isolate mutations that can rescue *CCM1* incompatibility

Sc-Ccm1 is a large protein (864 a.a.) and it only shares 72% protein identity with Sb-Ccm1. To dissect the molecular detail of *CCM1* incompatibility, we used an experimental evolution approach to isolate the mutations that could rescue the incompatibility. Single colonies of Sc + *Sb-CCM1* cells were used to initiate 98 independent cell cultures, and the cultures were continuously propagated in glycerol-containing medium (see Materials and Methods). Under this selective regime, cells containing spontaneous mutations that rescued the respiratory defects of Sc + *Sb-CCM1* would grow more quickly and be enriched in the population. After selection, only one colony with improved fitness was selected from each cell culture for further analysis. Therefore, mutations identified from each colony were likely to represent an independent event. We collected 94 mutant clones in total because four of the cell cultures were contaminated during the experiment.

Next, we crossed the mutant clones with an isogenic Sc + *Sb-CCM1*-ρ^0 strain in which mtDNA had been deleted and a different nutrient marker (*URA3*) was inserted next to the *Sb-CCM1* gene. The diploid cells were then induced to enter meiosis, and their tetrads were analyzed. If the suppressor mutation occurred in mtDNA, the spores would display a non-Mendelian 4:0 segregation pattern for improved respiration (Fig 3A). In contrast, a 2:2 segregation pattern would be observed if the rescue effect involved a single nuclear mutation. Since the two alleles of *Sb-CCM1* were next to different nutrient markers (*URA3* or *HIS3*), we could easily check whether the suppressor mutations co-segregated with the *Sb-CCM1* gene. The

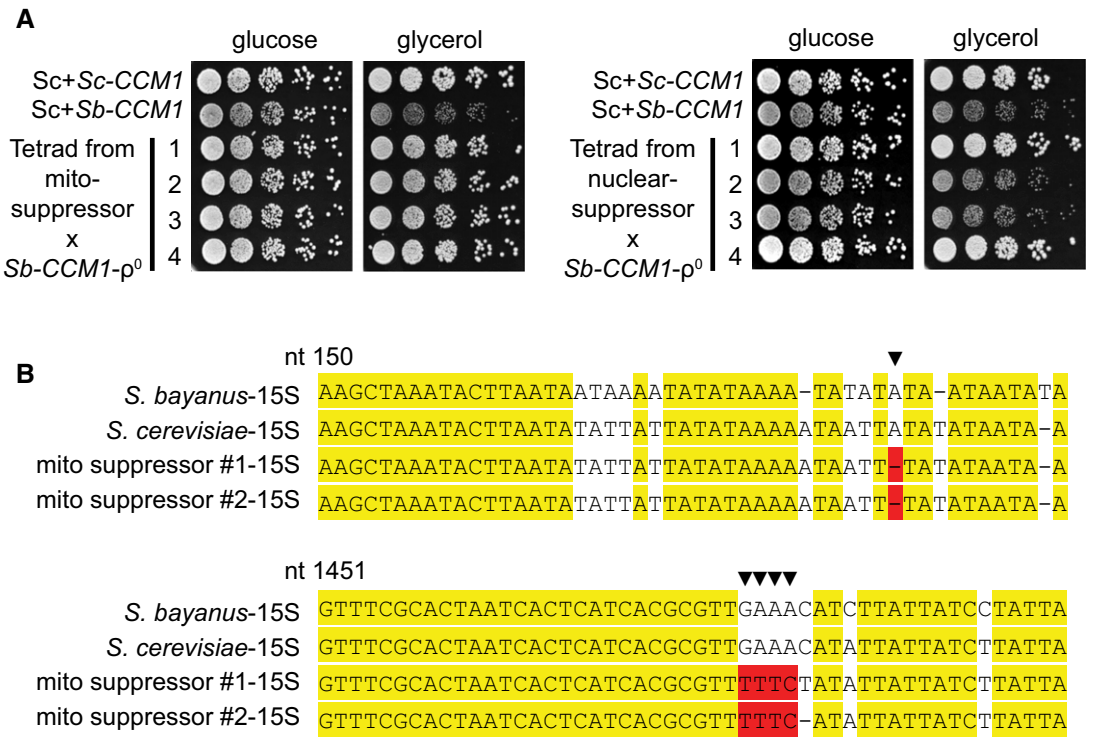

Figure 3. Incompatibility of *Sb-CCM1* can be relieved by mutations in the mitochondrial genome.

A Tetrad analysis reveals that the respiration defect of Sc + *Sb-CCM1* cells can be rescued by mutations in mitochondrial or nuclear genomes. The suppressor clones were crossed with the Sc + *Sb-CCM1*-ρ^0 strain and the tetrads from the cross were analyzed. A non-Mendelian 4:0 segregation pattern for improved respiration is expected if the suppressor mutation is in mtDNA (left panel). Otherwise, a 2:2 segregation pattern would be observed if the rescue effect involved a single nuclear mutation (right panel).

B Partial sequence alignment of 15S rRNA from *S. bayanus*, *S. cerevisiae*, and two mitochondrial suppressor clones (#1 and #2) of Sc + *Sb-CCM1*. A single nucleotide deletion at position 188 and four nucleotide substitutions at positions 1,524–1,527 found in both suppressor clones are labeled in red.

evolved *Sb-CCM1* gene was sequenced if it was linked with the suppressor mutation. Among 94 evolved clones, two clones carried mtDNA suppressors, 20 clones carried mutations in the *Sb-CCM1* gene, and the remainder contained mutations in unknown nuclear genes.

For those clones carrying mtDNA suppressors, the rescue effect was further confirmed by reintroducing their mtDNA into an ancestral Sc + *Sb-CCM1*-ρ^0 strain, indicating that no nuclear mutations were involved. Because our experiments had shown that *S. cerevisiae* 15S rRNA interacted with Sb-Ccm1 more weakly than its interaction with Sc-Ccm1, we directly sequenced evolved mitochondrial 15S rRNA to see whether it had been modified. Interestingly, both mitochondrial suppressor clones shared similar mutations, a single nucleotide deletion at position 188 and four nucleotide substitutions at positions 1,524–1,527 (Fig 3B). Although we cannot rule out the possibility that the rescue effects arose from unidentified mutations elsewhere in the evolved mtDNA, these results clearly show that the compatibility status of mito-nuclear interactions can be changed by evolving either side of the interaction.

Changes in the PPR domain of *Sb-CCM1* rescue the incompatibility

For the *Sb-CCM1* mutant clones, we first PCR-amplified the *Sb-CCM1* sequences from the suppressor genomes, reintroduced them into wild-type *S. cerevisiae* cells, and tested for their compatibility by growing the cells on glycerol plates. All the *Sb-CCM1* mutants were confirmed to have regained compatibility with the *S. cerevisiae* genome (Fig 4A). Interestingly, most of the mutations were *de novo* amino acid changes and only two mutants had changed their residues from the *S. bayanus* sequence to the *S. cerevisiae* sequence (*Sb-CCM1*^{F294L} and *Sb-CCM1*^{D400N}). Because the D residue at position 400 is conserved between *S. bayanus* and the outgroup species *Naumovia castellii*, and it has become N in *S. cerevisiae*, *S. paradoxus*, *S. mikatae*, and *S. kudriavzevii*, it suggests that the D and N residues probably represent the ancestral and derived amino acid states, respectively (Fig 4B). The unequivocal correlation between the compatibility and the amino acid states of the 400th residue in *S. cerevisiae* prompted us to test the importance of this residue in *S. bayanus*. Indeed, the D400N substitution, but not E375Q (a *de novo* substitution that repeatedly appeared in three independent clones), in *Sb-CCM1* caused a severe respiratory defect in *S. bayanus* (Fig 4C), suggesting that the 400th residue plays a determinant role in *S. cerevisiae*–*S. bayanus* incompatibility.

In the suppressor clones, several mutants (*Sb-CCM1*^{Q372H}, *Sb-CCM1*^{E375Q}, and *Sb-CCM1*^{E375K}) appeared multiple times, indicating that our suppressor screen was close to saturation. In total, 16 unique *Sb-CCM1* mutants were identified. When the structural positions of these suppressor mutations were further analyzed, it revealed the striking feature that all mutations were located at predicted PPR motifs (Fig 4D and Appendix Table S1 according to [41]). PPR domains have been speculated to provide the interface for RNA binding [46]. Our result shows that interactions between Ccm1 and 15S rRNA could be improved by modifying different PPR motifs, suggesting that the PPR motif is highly flexible.

The levels of mtDNA-encoded proteins and 15S rRNA are improved in the suppressor clones

In the Sc + *Sb-CCM1* strain, we have found that the weakened interaction between Sb-Ccm1 and *S. cerevisiae* 15S rRNA resulted in reduced levels of 15S rRNA and mtDNA-encoded Cox proteins. If the suppressor mutations rescued the *Sb-CCM1* incompatibility via improvements in RNA binding, the 15S rRNA level and thus mtDNA-encoded protein levels should be restored at least partially. We tested this idea by measuring the levels of 15S rRNA in two nuclear suppressor (*Sb-CCM1*^{D400N} and *Sb-CCM1*^{E375Q}) and one mitochondrial suppressor strains using quantitative PCR. Indeed, all three suppressor strains exhibited significant increments in 15S rRNA even though they have not reached the wild-type level (Fig 5A). To know whether the increased 15S rRNA levels were enough to rescue the defect in mitochondrial protein translation, we examined mtDNA-encoded Cox1, Cox2, and Cox3 using Western blots. The abundance of these proteins was significantly improved in the suppressor strains (Fig 5B). These data show that both nuclear and mitochondrial suppressors rescued the incompatibility through increased levels of 15S rRNA and mitochondrial protein translation.

Hybrid incompatibility caused by PPR proteins is prevalent among *Saccharomyces sensu stricto* yeast species

Pentatricopeptide repeat proteins belong to the largest RNA-binding protein family in eukaryotes that function mostly in mitochondria or chloroplasts [46]. In the *S. cerevisiae* genome, there are 15 predicted PPR genes. Previously, it has been speculated that genes involved in hybrid incompatibility may evolve more rapidly [52]. We calculated the evolutionary rates of PPR proteins together with other protein families that shared similar features, including the MRP (required for mitochondrial protein translation), TRP (proteins with repetitive tandem motifs), RRM, and PUF (RNA-binding proteins) families. Interestingly, only PPR proteins exhibited significantly increased evolutionary rates (Fig 6A and Appendix Fig S1).

Yeast mtDNA is highly dynamic in its genome structure and has much higher base substitution rates than the nuclear genome [20,53–55]. If co-evolution between mitochondrial RNA and the RNA-binding PPR protein led to the observed high evolutionary rates of PPR proteins, PPR proteins might have a higher chance to develop genetic incompatibility among closely related yeast species. We used functional assays to investigate whether PPR genes other than *CCM1* and *AEP2* also contribute to hybrid incompatibility among *Saccharomyces sensu stricto* yeast species. In order to detect the mito-nuclear incompatibility caused by PPR genes, we first crossed the *S. cerevisiae* mutant strains lacking individual PPR genes with mtDNA-less strains of *S. paradoxus*, *S. mikatae*, *S. kudriavzevii*, and *S. bayanus*, and examined their growth in glycerol-containing medium. If any growth defect was observed in the hybrid diploids, we further validated the incompatibility by expressing the orthologous alleles in the *S. cerevisiae* deletion strains (see Materials and Methods). One of the PPR genes, *RMD9L*, showed no detectable growth defects in glycerol-containing medium when deleted in *S. cerevisiae*. Therefore, this gene was excluded from our assays. We examined 12 additional PPR genes and found that seven of them (*AEP1*, *AEP3*, *MRX1*,

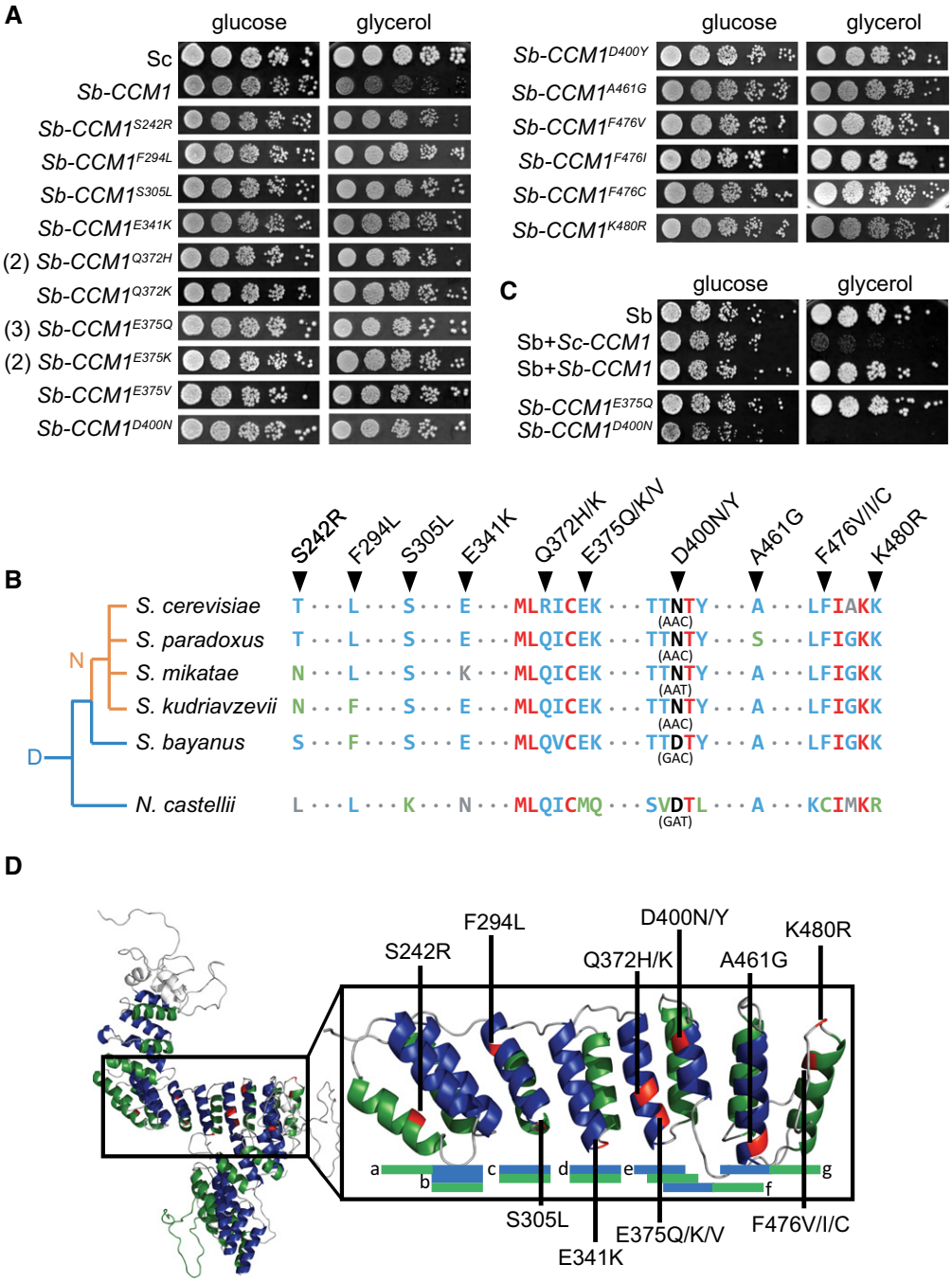

Figure 4. Changes in the PPR domain of *Sb-CCM1* rescue the incompatibility.

A Reconstituted *Sb-CCM1* mutants can rescue the incompatibility of *Sb-CCM1*. Among 94 suppressor clones, 20 of them carry mutations in the *Sb-CCM1* gene. These mutants were reconstructed in Sc + *Sb-CCM1* cells to test their function. Superscripts next to *Sb-CCM1* indicate the respective amino acid substitutions, and numbers in parentheses indicate the number of independent clones in our suppressor screen. Sc, wild-type *S. cerevisiae*.

B Sequence alignment shows that most of the *Sb-CCM1* suppressor mutants contain *de novo* amino acid changes and only two mutants have switched their residues from the *S. bayanus* sequence to the *S. cerevisiae* sequence (F294L and D400N). Letters beside the phylogenetic tree (in which the line lengths are not proportional to the evolutionary distances) indicate the amino acid state at the 400th residue and parentheses contain the codons encoding for the amino acids.

C The 400th residue plays a determinant role in the *S. cerevisiae–S. bayanus* incompatibility. Both *Sb-CCM1*^{E375Q} and *Sb-CCM1*^{D400N} mutants relieved the incompatibility in *S. cerevisiae*, but only *Sb-CCM1*^{D400N} caused respiration defects in *S. bayanus*. The *Sb-CCM1*^{E375Q} mutant was selected as a control in this experiment since it was a charged-to-polar substitution similar to *Sb-CCM1*^{D400N} and also appeared three times in our screen. Sb, wild-type *S. bayanus*.

D Protein structural analysis shows that all intramolecular suppressor mutations were located on the predicted PPR motifs. The predicted protein structure of Ccm1 is shown on the left. Blue and green colors indicate the two α-helices in each predicted PPR motif and white color indicates additional α-helices in the N-terminus and the middle region. Red color indicates the positions of the suppressor mutations. Predicted PPR motifs occupy around 52% of the whole protein (453 of 871 residues). The box on the right displays a magnified version of some PPR motifs where the substitutions are located.

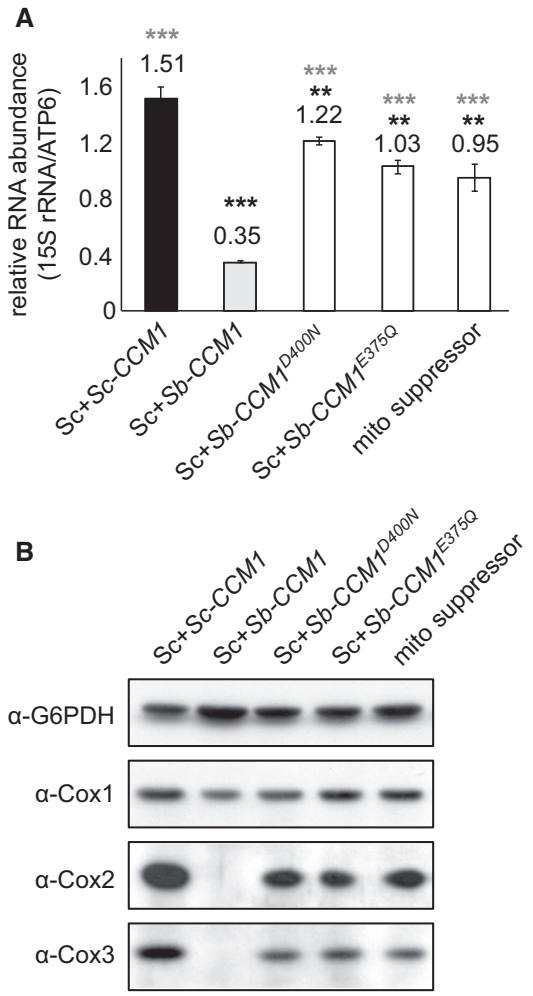

Figure 5. Suppressor mutations partially restored the levels of 15S rRNA and mtDNA-encoded proteins.

A 15S rRNA levels are increased in the suppressor clones. Total RNA was isolated from the replacement strains (Sc + *Sc-CCM1* and Sc + *Sb-CCM1*), two nuclear suppressor strains (Sc + *Sb-CCM1*^{D400N} and *Sc + Sb-CCM1*^{E375Q}), and one mitochondrial suppressor strain and then subjected to quantitative PCR analyses. Relative mRNA abundance was calculated by normalizing the 15S rRNA level to the *ATP6* mRNA level. Graph was plotted using data from five independent repeats for each strain, and *P*-values were calculated by unpaired, two-sided Student's *t*-test. Error bars indicate SD. ***P-value < 0.001. **P-value < 0.01. Asterisks in black, comparing Sc + *Sc-CCM1* with others. Asterisks in gray, comparing Sc + *Sb-CCM1* with others.

B The steady-state level of mtDNA-encoded proteins is increased in the suppressor clones. Protein extracts from the replacement and suppressor strains were hybridized with antibodies against G6PDH, Cox1, Cox2, or Cox3.

PET111, *PET309*, *RPM2*, and *RPO41*) displayed various levels of incompatibility between *S. cerevisiae* and at least one *Saccharomyces sensu stricto* species (Fig 6B and Table 1). In total, nine out of 14 PPR genes in the yeast genome have evolved incompatibility among these closely related yeast species. As a control, we also tested six MRP genes under the same conditions and observed no discernible incompatibility (Appendix Table S2). These results suggest that mitochondrial–nuclear incompatibility is prevalent among *Saccharomyces sensu stricto* yeast species and the highly evolvable PPR proteins may have a major contributory role in the evolution of hybrid incompatibility.

Discussion

The general rules underlying the development of hybrid incompatibility remain unclear despite several incompatibility genes having been identified and characterized during the past decade [10]. Nonetheless, it appears that incompatibilities between nuclear and organellar genomes is a widespread phenomenon across multiple eukaryotic kingdoms [12]. Previously, two genes encoding mitochondrial RNA-binding proteins have been identified to cause mitochondrial–nuclear incompatibility among closely related yeast species [29,36]. In the current study, we further demonstrate that about two-thirds of budding yeast PPR proteins have evolved incompatibility among the *Saccharomyces sensu stricto* yeasts. Together with the observation that PPR proteins exhibit a higher evolutionary rate not found in other RNA-binding proteins, it suggests that PPR proteins may play a specific role in the development of hybrid incompatibility.

Pentatricopeptide repeat proteins were first discovered in plants and had expanded dramatically during the evolution of land plants [46,56]. Studies indicate that these PPR proteins are involved in various aspects of RNA processing [42]. Co-evolution between plant PPR proteins and organellar genomes has been demonstrated [57,58], and consistent with yeast PPR proteins, these plant PPR proteins are also fast-evolving [59–61]. The role of PPR proteins in hybrid incompatibility was previously demonstrated in cytoplasmic male sterility (CMS) in hybrid plants [62,63]. CMS is caused by aberrant recombinant events in the mtDNA and can be rescued by nucleus-encoded restorer of fertility (Rf) genes [31,64]. Several Rf genes have been shown to belong to the PPR protein family [65,66]. In a study of *Mimulus* species, two linked loci responsible for hybrid incompatibility were found to contain a large number of recently expanded PPR genes, and these genes showed high homology to restorers in distantly related taxa [64]. These findings suggest that plant PPR genes co-evolved with mtDNA to control its abnormal behavior [65–67].

Pentatricopeptide repeat motifs act in a coordinated manner; each base of the RNA target is recognized by two consecutive PPR motifs [43–45]. Our suppressor screen revealed how rapidly the *CCM1* gene can reclaim compatibility when encountering an incompatible foreign mtDNA (Fig 4). Importantly, substitutions capable of rescuing incompatibility need not be located on a specific PPR motif, further supporting the idea that the coordinated action of PPR motifs might exert an intramolecular buffering effect to increase the flexibility of PPR proteins [41]. One possible scenario is that the flexibility of PPR proteins allows a population to accumulate more mutations in the PPR genes, and such genetic variation further enables cells to tolerate changes in the RNA targets of PPR proteins resulting from genetic drift or selection. However, if co-evolutionary processes are driven in different directions between two populations, incompatibility caused by mismatched PPR genes and RNA targets may eventually occur in hybrids.

Dysfunctional mitochondria have been implicated in many human diseases, including neuronal degeneration and cancer

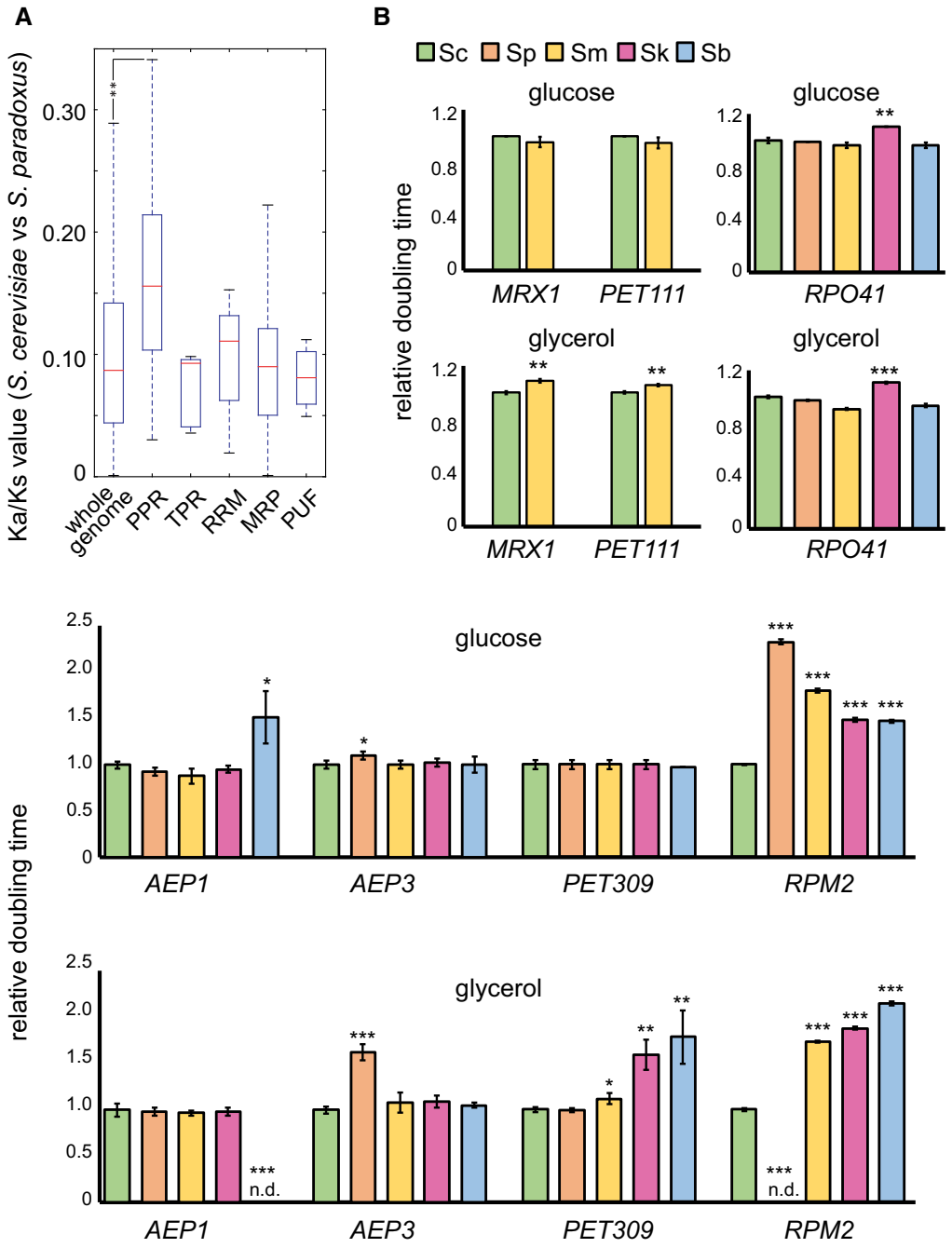

Figure 6. Many PPR genes evolve hybrid incompatibility in *Saccharomyces sensu stricto* yeasts.

A PPR genes show significantly increased evolutionary rates. Box plot of the evolutionary rates (Ka/Ks) of PPR, TPR, RRM, MRP, and PUF genes and the whole genome by comparing *S. cerevisiae* and *S. paradoxus*. All these protein families share some features with the PPR proteins. TPR proteins contain TPR motifs that share a similar repetitive structure with the PPR motifs but mainly mediate protein–protein interactions [94]. RRM proteins are RNA recognition motif-containing proteins and function in splicing, RNA stability, and translation [95]. MRP proteins comprise ribosomal proteins encoded in the nuclear genome that are imported into the mitochondria [96]. PUF proteins contain RNA-binding motifs similar to the PPR motifs and are involved in mRNA posttranscriptional events, including mitochondrial import of mRNA [97]. *P*-values were calculated by two-sample Kolmogorov–Smirnov test. ***P*-value = 7.0143E-3. The bottom and top of the box are the first and third quartiles of the data, and the red band inside is the median. The ends of the whiskers represent the lowest and highest data points within 1.5 interquartile range of the lower and upper quartiles, respectively.

B Seven of the 12 tested PPR genes exhibit incompatibility between *S. cerevisiae* and at least one other *Saccharomyces sensu stricto* species. The doubling time of *S. cerevisiae* cells carrying the endogenous PPR genes (Sc) or orthologs of other yeast species (Sp, Sm, Sk, and Sb) were measured in YPD (glucose) or YPG (glycerol) media. All the measurements were then normalized to the doubling time of Sc to obtain the relative doubling time. Graphs were plotted using data from at least three independent repeats for each strain. Sc, *S. cerevisiae*. Sp, *S. paradoxus*. Sm, *S. mikatae*. Sk, *S. kudriavzevii*. Sb, *S. bayanus*. n.d., growth not detected. *P*-values were calculated by unpaired, two-sided Student's *t*-test. Error bars indicate SD. **P*-value < 0.05. ***P*-value < 0.01. ****P*-value < 0.001.

[68,69]. Intriguingly, many pathogenic mutations detected in genome-wide association studies (GWAS) are also found as sequence variants in normal populations [70–72], raising the possibility that some pathogenic mutations may have been maintained through the process of mitochondrial–nuclear co-evolution. Indeed, compromised mitochondrial functions have been experimentally demonstrated using human cybrid cells in which mtDNA variants are combined with different nuclear backgrounds [73,74]. In a recent study, it was further shown that mice with mismatched mitochondrial and nuclear genomes exhibit disturbed organismal metabolic performance and aging [75]. These observations suggest that mitochondrial–nuclear incompatibilities might already exist in human populations and contribute to the observed mitochondrial disorders.

It is often speculated that the high mutation rate of mtDNA is the major force driving the evolution of mitochondrial–nuclear incompatibility; when deleterious mutations in mtDNA are fixed in the population by genetic drift, compensatory nuclear mutations will be selected to rescue the fitness. Such co-evolutionary processes will eventually differentiate a population from its ancestor or other populations in which co-evolution is taking different trajectories [21–23,26,30]. However, it has recently been suggested that more complicated interactions, such as genomic conflicts, may speed up the co-evolutionary process between mitochondrial and nuclear genomes [9,55]. As the replication of mtDNA is autonomous—replicating independently of the cell cycle—mutations that expedite mtDNA replication or that directly act on transmission to daughter cells will spread into the population even if they are not beneficial to the host. Moreover, because the inheritance of mtDNA is mainly asexual, whatever deleterious mutations occur in selfish mtDNA will hitchhike with it. Similar to the mutation accumulation model, host genomes need to offset these selfish or deleterious mutations to prevent the population from extinction. Nonetheless, the whole process is much faster than genetic drift, because the spread of mtDNA mutations in the first instance is driven by selection [55].

While the high mutation rate or selfish behavior of mtDNA constantly threatens the stability of the symbiotic relationship between mitochondrial and nuclear genomes, the highly flexible PPR proteins might represent a special defense system of the host cell. In yeast, two-thirds of PPR proteins have changed to accommodate alterations of their RNA targets in mitochondria during the

Table 1. Genetic incompatibility of PPR genes among *Saccharomyces cerevisiae* and other *Saccharomyces sensu stricto* yeasts.

Protein	Location	Function[a]	Mitochondrial target[a]	Incompatibility	Incompatible species	References
Aep1	Chr 13	Translation of *ATP9*	*ATP9*	Strong[b,c]	*S. bayanus*	[47]
Aep2	Chr 13	Translation of *ATP9*	*ATP9*	Strong[d]	*S. bayanus*	[29,47]
Aep3	Chr 16	Stabilization of *ATP6/8*	*ATP6/8*	Mild[b,c]	*S. paradoxus*	[47]
Atp22	Chr 4	Translation of *ATP6/8*	*ATP6/8*	No[b,c]		[47]
Pet309	Chr 12	Stabilization and translation of *COX1*	*COX1*	Mild[b,c]	*S. mikatae* *S. kudriavzevii* *S. bayanus*	[47]
Ccm1	Chr 7	Stabilization of 15S rRNA Processing of *COX1*, *COB*	*15S rRNA* *COX1*, *COB*	Mild[b,c]	*S. bayanus*	[47,49–51]
Cbp1	Chr 10	Stabilization and translation of *COB*	*COB*	No[b,c]		[47]
Pet111	Chr 13	Translation of *COX2*	*COX2*	Weak[b,c]	*S. mikatae*	[47]
Rmd9	Chr 7	Delivering into ribosomes	All mRNAs?	No[c]		[47]
Rpm2	Chr 13	Mitochondrial RNase P	All tRNAs	Strong[c,e]	*S. paradoxus* *S. mikatae* *S. kudriavzevii* *S. bayanus*	[47]
Rpo41	Chr 6	Mitochondrial RNA polymerase	All RNAs	Weak[c]	*S. kudriavzevii*	[47]
Sov1	Chr 13	Unknown; mutant is defective in mitochondrial respiration	*VAR1*	No[b]		[47]
Rmd9L	Chr 2	Processing/stability of mitochondrial mRNAs; mutant is not defective in mitochondrial respiration	All mRNAs?	n.d.		[47]
Msc6	Chr 15	Multicopy suppressor of *her2* involved in mitochondrial translation	Unknown	No[b]		[47,98]
Mrx1	Chr 5	Organization of mitochondrial gene expression	Unknown	Weak[b,c]	*S. mikatae*	[47,98]

n.d., not determined since corresponding deletion strain has no respiratory defect.
[a]Information obtained from the reference.
[b]Evaluated via complementation assays.
[c]Evaluated via plasmid assays.
[d]Previous report.
[e]Showing strong defects in both glucose and glycerol media.

recent divergence in *Saccharomyces sensu stricto* species. The Rf genes in plants provide further evidence that PPR proteins are able to counteract the selfish behavior of mtDNA [64,66]. PPR proteins have been identified in fungi, plants, and animals [41,46,76]. Although mtDNA sizes vary significantly between different eukaryotic lineages, complicated mitochondrial RNA regulation has been observed even in human cells that carry very small mtDNA (consisting of only 16 kb) [77,78]. This may explain why cells employ the versatile RNA regulatory functions of PPR proteins to control mtDNA. In the future, it will be interesting to see how PPR proteins co-evolve with their targets in other eukaryotic lineages since different types of mtDNA may have distinct mutation patterns or behaviors. In addition, dissecting the evolutionary trajectories of PPR proteins and their mtDNA targets will shed light on the underlying driving force in the evolution of mitochondrial–nuclear incompatibility.

Materials and Methods

Yeast strains and genetic procedures

Yeast strain genotypes are listed in Appendix Table S3. The *S. cerevisiae* haploid strains were derived from W303 (*MATa ura3-1 his3-11,15 leu2-3,112 trp1-1 ade2-1 can1-100*). The parental *S. bayanus* strains were derived from a strain (*S. bayanus* #180) collected by Dr. Duccio Cavalieri (University of Florence, Italy). The parental *S. paradoxus*, *S. mikatae*, and *S. kudriavzevii* strains were derived from YDG197, YDG193, and YDG190, respectively, and are gifts from Dr. Duncan Greig (University College London, UK). The chromosome 7 replacement strain (Sc + Sb-chr7) was constructed in a previous study [29]. Strains carrying TAP-tagged proteins were from the yeast TAP-tagged ORF collection [79]. Substitutive and integrative transformations were carried out by the lithium acetate procedure [80]. Heat-shock treatments of yeast transformation for *S. cerevisiae* and *S. bayanus* were 15 min at 42°C and 30 min at 37°C, respectively. Media, microbial, and genetic techniques were as described [81].

For *CCM1* orthologous allele replacements, we PCR-amplified the coding region with around 500 bp upstream and 500 bp downstream flanking sequences of the *CCM1* gene, and a *HIS3* gene serving as the selection marker. These fragments were then fused using PCR and transformed into wild-type cells using lithium acetate procedure. Successful recombinants were selected on CSM-HIS plates and verified by PCR and sequencing. In the *Sb-CCM1* overexpression experiment, *Sb-CCM1* with around 1,000 bp upstream and 500 bp downstream flanking sequences was PCR-amplified with a ATGCGGATCC overhanging on both ends and cloned into a 2-micron multi-copy plasmid (pRS426) at the BamHI cutting site via ligation. The plasmid was then overexpressed in the Sc + *Sb-CCM1* strain. To validate the compatibility of different PPR genes, orthologous alleles with around 1,000 bp upstream and 500 bp downstream flanking sequences were PCR-amplified and cloned into a single-copy plasmid (pRS416) via yeast *in vivo* recombination. The plasmids were then transformed into the strain with the gene deleted.

To generate yeast strains lacking mtDNA (ρ^0 strains), the cells were inoculated in YPD containing 25 μg/ml of ethidium bromide and cultured overnight [82]. The cells were then spread on YPD plates to form single colonies and replica-plated on glycerol-containing plates to test their respiratory capability. All petite strains were further examined under a microscope using DAPI (4′,6-diamidino-2-phenylindole) staining.

Genomic DNA library screen

The chromosome 7 replacement strain was transformed with a genomic DNA library comprising most of the ORFs of *S. cerevisiae* carried on the pRS416 CEN plasmid. To construct the genomic DNA library, genomic DNA from wild-type *S. cerevisiae* cells was partially digested with Sau3AI to yield fragments of around 2.5–10 kb, and then cloned into the pRS416 CEN plasmid previously cut with BamHI. Transformants were grown on CSM-URA + glycerol plates, and only colonies with obviously improved growth rates were selected. The selected colonies were further tested to see whether the improved respiratory growth depended on the plasmid. The plasmid exhibiting rescue ability was isolated from the cells, and the insertion fragment was identified by Sanger sequencing.

Subcellular fractionation and Western blot analyses

Yeast cells were cultured in selection medium at 30°C to the late-exponential phase. Mitochondrial fractions were prepared as described [83]. Briefly, cells were pretreated with Tris-SO_4 buffer (containing 100 mM Tris-SO_4 and 10 mM dithiothreitol; pH 9.4) at 30°C for 10 min under agitation (~140 rpm) and then treated with Zymolyase 20T (2 mg/g cell wet weight) in 1.2 M sorbitol buffer (containing 20 mM phosphate buffer; pH 7.4) at 30°C for 20–40 min under agitation (~140 rpm). The cells were then homogenized by vortex (max intensity) with glass beads for 10 min (30-s on and 30-s off cycles) in 0.6 M sorbitol buffer (containing 20 mM HEPES-KOH; pH 7.4; RNase inhibitor (Qiagen, Valencia, CA, USA) and protease inhibitor cocktail (Set III, EDTA-free; Calbiochem, San Diego, CA, USA) were added shortly before use). Cell debris and the glass beads were removed by centrifugation at 2,000 *g* for 5 min. The cytosolic and mitochondrial fractions were separated by centrifugation at 12,000 *g* for 10 min repeatedly. The postmitochondrial supernatant (PMS) fractions were collected immediately following centrifugation of mitochondria. Laemmli sample buffer was added to the mitochondrial pellets resuspended in TE buffer plus protease inhibitors, and to the PMS fractions.

For Western blot analyses, mitochondrial protein (40 μg) was separated by SDS–PAGE using the GE Healthcare Life Science system (Mini-Vertical Units SE260) and then transferred to a Bio-Rad Immun-Blot PVDF membrane in transfer buffer (25 mM Tris base, 200 mM glycine, 25% methanol). The immunopositive bands were visualized by using Western Lightning Chemiluminescence Reagent (PerkinElmer, Waltham, MA, USA). Anti-G6PDH antibody was purchased from Sigma (St. Louis, MO, USA). Anti-c-Myc antibody (sc-40) was from Santa Cruz Biotechnology (Dallas, TX, USA) and anti-TAP antibody (CAB1001) was from Thermo Fisher Scientific (Waltham, MA, USA). Anti-Cox1 (MS418), anti-Cox2 (MS419), and anti-Cox3 (MS406) were purchased from MitoScience, Abcam (Cambridge, UK).

RNA isolation and Northern analyses of mitochondrial transcripts

Yeast strains were grown in 3 ml YPD liquid cultures at 30°C to stationary phase, and total RNA was isolated using Qiagen RNeasy Midi Kits (Qiagen, Valencia, CA, USA). Ten micrograms of total RNA was separated on a 1.3% agarose–formaldehyde gel and then transferred to a nylon membrane (Millipore, Billerica, MA, USA). Northern blotting was performed as described [84]. Probe generation and hybridization were as described in the Genius System User's Guide (Roche, Indianapolis, IN, USA). The gene-specific primers for the DIG-labeled probes for *COX1*, *COX3*, *COB*, and *COX2* were described in previous studies [36,85]. We used 3′ end-DIG-labeled oligo-nucleotide probes for 15S rRNA [50], 21S rRNA [86], and *ATP6/8* [87].

RNA immunoprecipitation and quantitative PCR

RNA immunoprecipitation was performed following Selth *et al.* [88]. Briefly, 100 ml of yeast cells carrying *Sc-CCM1*, *Sc-CCM1-13Myc*, or *Sb-CCM1-13Myc* was first treated with formaldehyde to generate protein–RNA cross-links, and mitochondrial fractions were prepared as described above. The mitochondrial fractions were then incubated with anti-Myc agarose beads (A7470; Sigma-Aldrich) at 4°C overnight. After immunoprecipitation and cross-link reversal, RNAs were phenol–chloroform-extracted from the elute, reverse-transcribed by random hexamer, and quantified using an Applied Biosystems 7500 Fast Real-Time PCR machine (Applied Biosystems, Foster City, CA, USA). Enrichment was calculated using the formula $2^{[(CT_{sample-input}-CT_{sample-elute})-(CT_{control-input}-CT_{control-elute})]}$.

Experimental evolution for the *Sb-CCM1* suppressors

Single colonies of the Sc + *Sb-CCM1* cells were used to initiate independent cultures in 3 ml of the selective medium and cultured at 30°C overnight. 50 μl of the overnight cultures was transferred to new tubes containing 5 ml of YEP + glycerol and cultured for 1 week in each cycle. The heterogeneity of the cultures was then examined using spot assays. The same experimental cycle was repeated twice until suppressors became predominant in the population. Evolved cells were spread on YEP + glycerol plates to form single colonies. Only a single colony with improved fitness was collected from each evolved culture and subjected to further genetic characterization to determine whether the suppressors were located in mtDNA, *Sb-CCM1*, or other loci in the nuclear genome. Genetic analysis revealed that among the clones carrying unknown nuclear mutations, 13 of them contained multiple mutations contributing to the suppressor phenotypes.

Protein structure prediction

The Ccm1 protein structures were predicted by the Raptor X server using default settings [89–92]. Colors and labels were manually added using the PyMOL program (The PyMOL Molecular Graphics System, version 1.7.4 Schrödinger, LLC.).

Evolutionary rate analysis

Evolutionary rates were represented by Ka values (for comparisons between *S. cerevisiae* and *C. glabrata* or *N. castellii*) or Ka/Ks values (for comparisons between *Saccharomyces sensu stricto* yeast species). The Ka and Ks values were computed by the CodeML program of the PAML package [93]. Significance of differences in evolutionary rates between each group of genes and the whole genome was tested by the Kolmogorov–Smirnov test.

Growth rate measurements

Cells were cultured in YPD at permissive temperatures (28°C for *S. cerevisiae* and 23°C for *S. bayanus*; when cultured together, 28°C was used) overnight before assessment. For spot assays, cell densities were adjusted to 625 cells/μl and fivefold serially diluted four times, and 3 μl of the resulting suspension was added onto the YPD and YEP + glycerol plates. To measure the doubling time, overnight cell cultures were diluted 10-fold in fresh medium for 3 h and then the cell densities were adjusted to OD_{600} = 0.05 to start the measurement. The OD values were recorded for 72 h using Infinite 200 series plate readers (Tecan, Mannedorf, Switzerland) with continuous shaking, and then, the doubling times were estimated using homemade Python scripts (available on request).

Expanded View for this article is available online.

Acknowledgements
We thank members of the Leu laboratory for helpful discussion and comments on the manuscript. We also thank John O'Brien for manuscript editing. This work was supported by Academia Sinica of Taiwan (grant no. 2316-1050-300) and the Taiwan Ministry of Science and Technology (105-2321-B-001-030).

Author contributions
J-YL and H-YJ conceived the study. H-YJ, H-YL, and J-YL designed analyses and interpreted results. H-YJ, H-YL, and J-YL performed the experiments. H-YJ and J-YL wrote the manuscript.

Conflict of interest
The authors declare that they have no conflict of interest.

References

1. Greig D (2009) Reproductive isolation in Saccharomyces. *Heredity* 102: 39 – 44
2. Hou J, Schacherer J (2016) Negative epistasis: a route to intraspecific reproductive isolation in yeast? *Curr Genet* 62: 25 – 29
3. Leducq JB, Nielly-Thibault L, Charron G, Eberlein C, Verta JP, Samani P, Sylvester K, Hittinger CT, Bell G, Landry CR (2016) Speciation driven by hybridization and chromosomal plasticity in a wild yeast. *Nat Microbiol* 1: 15003
4. Louis EJ (2011) Population genomics and speciation in yeasts. *Fungal Biol Rev* 25: 136 – 142
5. Zanders SE, Eickbush MT, Yu JS, Kang JW, Fowler KR, Smith GR, Malik HS (2014) Genome rearrangements and pervasive meiotic drive cause hybrid infertility in fission yeast. *Elife* 3: e02630
6. Orr HA, Masly JP, Presgraves DC (2004) Speciation genes. *Curr Opin Genet Dev* 14: 675 – 679
7. Dobzhansky T (1937) *Genetics and the origin of species*. New York: Columbia University Press

8. Presgraves DC (2010) The molecular evolutionary basis of species formation. *Nat Rev Genet* 11: 175 – 180
9. Johnson NA (2010) Hybrid incompatibility genes: remnants of a genomic battlefield? *Trends Genet* 26: 317 – 325
10. Maheshwari S, Barbash DA (2011) The genetics of hybrid incompatibilities. *Annu Rev Genet* 45: 331 – 355
11. Chou JY, Leu JY (2010) Speciation through cytonuclear incompatibility: insights from yeast, and implications for higher eukaryotes. *BioEssays* 32: 401 – 411
12. Burton RS, Pereira RJ, Barreto FS (2013) Cytonuclear genomic interactions and hybrid breakdown. *Annu Rev Ecol Evol Syst* 44: 281 – 302
13. Gershoni M, Templeton AR, Mishmar D (2009) Mitochondrial bioenergetics as a major motive force of speciation. *BioEssays* 31: 642 – 650
14. McBride HM, Neuspiel M, Wasiak S (2006) Mitochondria: more than just a powerhouse. *Curr Biol* 16: R551 – R560
15. Saccone C, Gissi C, Lanave C, Larizza A, Pesole G, Reyes A (2000) Evolution of the mitochondrial genetic system: an overview. *Gene* 261: 153 – 159
16. Blanchard JL, Lynch M (2000) Organellar genes: why do they end up in the nucleus? *Trends Genet* 16: 315 – 320
17. Allen JF, Raven JA (1996) Free-radical-induced mutation vs redox regulation: costs and benefits of genes in organelles. *J Mol Evol* 42: 482 – 492
18. Adams KL, Palmer JD (2003) Evolution of mitochondrial gene content: gene loss and transfer to the nucleus. *Mol Phylogenet Evol* 29: 380 – 395
19. Burger G, Gray MW, Lang BF (2003) Mitochondrial genomes: anything goes. *Trends Genet* 19: 709 – 716
20. Lynch M, Sung W, Morris K, Coffey N, Landry CR, Dopman EB, Dickinson WJ, Okamoto K, Kulkarni S, Hartl DL, *et al* (2008) A genome-wide view of the spectrum of spontaneous mutations in yeast. *Proc Natl Acad Sci USA* 105: 9272 – 9277
21. Schmidt TR, Wu W, Goodman M, Grossman LI (2001) Evolution of nuclear- and mitochondrial-encoded subunit interaction in cytochrome c oxidase. *Mol Biol Evol* 18: 563 – 569
22. Rawson PD, Burton RS (2002) Functional coadaptation between cytochrome c and cytochrome c oxidase within allopatric populations of a marine copepod. *Proc Natl Acad Sci USA* 99: 12955 – 12958
23. Barreto FS, Burton RS (2013) Evidence for compensatory evolution of ribosomal proteins in response to rapid divergence of mitochondrial rRNA. *Mol Biol Evol* 30: 310 – 314
24. Chang CC, Rodriguez J, Ross J (2016) Mitochondrial-nuclear epistasis impacts fitness and mitochondrial physiology of interpopulation caenorhabditis briggsae hybrids. *G3: Genes - Genomes - Genetics* 6: 209 – 219.
25. Bar-Yaacov D, Hadjivasiliou Z, Levin L, Barshad G, Zarivach R, Bouskila A, Mishmar D (2015) Mitochondrial involvement in vertebrate speciation? The case of mito-nuclear genetic divergence in chameleons. *Genome Biol Evol* 7: 3322 – 3336
26. Paliwal S, Fiumera AC, Fiumera HL (2014) Mitochondrial-nuclear epistasis contributes to phenotypic variation and coadaptation in natural isolates of *Saccharomyces cerevisiae*. *Genetics* 198: 1251 – 1265
27. Spirek M, Polakova S, Jatzova K, Sulo P (2014) Post-zygotic sterility and cytonuclear compatibility limits in *S. cerevisiae* xenomitochondrial cybrids. *Front Genet* 5: 454 .
28. Hou J, Friedrich A, Gounot JS, Schacherer J (2015) Comprehensive survey of condition-specific reproductive isolation reveals genetic incompatibility in yeast. *Nat Commun* 6: 7214
29. Lee HY, Chou JY, Cheong L, Chang NH, Yang SY, Leu JY (2008) Incompatibility of nuclear and mitochondrial genomes causes hybrid sterility between two yeast species. *Cell* 135: 1065 – 1073
30. Meiklejohn CD, Holmbeck MA, Siddiq MA, Abt DN, Rand DM, Montooth KL (2013) An incompatibility between a Mitochondrial tRNA and Its nuclear-encoded tRNA synthetase compromises development and fitness in *Drosophila*. *PLoS Genet* 9: e1003288
31. Luo D, Xu H, Liu Z, Guo J, Li H, Chen L, Fang C, Zhang Q, Bai M, Yao N, *et al* (2013) A detrimental mitochondrial-nuclear interaction causes cytoplasmic male sterility in rice. *Nat Genet* 45: 573 – 577
32. Ma H, Marti Gutierrez N, Morey R, Van Dyken C, Kang E, Lee Y, Li Y, Tippner-Hedges R, Wolf DP, Laurent LC, *et al* (2016) Incompatibility between nuclear and mitochondrial genomes contributes to an interspecies reproductive barrier. *Cell Metab* 24: 283 – 294.
33. Kreike J, Schulze M, Pillar T, Korte A, Rodel G (1986) Cloning of a nuclear gene MRS1 involved in the excision of a single group I intron (bI3) from the mitochondrial COB transcript in *S. cerevisiae*. *Curr Genet* 11: 185 – 191
34. Bousquet I, Dujardin G, Poyton RO, Slonimski PP (1990) Two group I mitochondrial introns in the cob-box and coxI genes require the same MRS1/PET157 nuclear gene product for splicing. *Curr Genet* 18: 117 – 124
35. Herbert CJ, Macadre C, Becam AM, Lazowska J, Slonimski PP (1992) The MRS1 gene of *S. douglasii*: co-evolution of mitochondrial introns and specific splicing proteins encoded by nuclear genes. *Gene Expr* 2: 203 – 214
36. Chou JY, Hung YS, Lin KH, Lee HY, Leu JY (2010) Multiple molecular mechanisms cause reproductive isolation between three yeast species. *PLoS Biol* 8: e1000432
37. Marvin ME, Williams PH, Cashmore AM (2001) The isolation and characterisation of a *Saccharomyces cerevisiae* gene (LIP2) involved in the attachment of lipoic acid groups to mitochondrial enzymes. *FEMS Microbiol Lett* 199: 131 – 136
38. Miller JR, Busby RW, Jordan SW, Cheek J, Henshaw TF, Ashley GW, Broderick JB, Cronan JE Jr, Marletta MA (2000) Escherichia coli LipA is a lipoyl synthase: *in vitro* biosynthesis of lipoylated pyruvate dehydrogenase complex from octanoyl-acyl carrier protein. *Biochemistry* 39: 15166 – 15178
39. Schonauer MS, Kastaniotis AJ, Kursu VA, Hiltunen JK, Dieckmann CL (2009) Lipoic acid synthesis and attachment in yeast mitochondria. *J Biol Chem* 284: 23234 – 23242
40. Finnegan PM, Payne MJ, Keramidaris E, Lukins HB (1991) Characterization of a yeast nuclear gene, AEP2, required for accumulation of mitochondrial mRNA encoding subunit 9 of the ATP synthase. *Curr Genet* 20: 53 – 61
41. Lipinski KA, Puchta O, Surendranath V, Kudla M, Golik P (2011) Revisiting the yeast PPR proteins–application of an Iterative Hidden Markov Model algorithm reveals new members of the rapidly evolving family. *Mol Biol Evol* 28: 2935 – 2948
42. Fujii S, Small I (2011) The evolution of RNA editing and pentatricopeptide repeat genes. *New Phytol* 191: 37 – 47
43. Barkan A, Rojas M, Fujii S, Yap A, Chong YS, Bond CS, Small I (2012) A combinatorial amino acid code for RNA recognition by pentatricopeptide repeat proteins. *PLoS Genet* 8: e1002910
44. Takenaka M, Zehrmann A, Brennicke A, Graichen K (2013) Improved computational target site prediction for pentatricopeptide repeat RNA editing factors. *PLoS One* 8: e65343
45. Coquille S, Filipovska A, Chia T, Rajappa L, Lingford JP, Razif MF, Thore S, Rackham O (2014) An artificial PPR scaffold for programmable RNA recognition. *Nat Commun* 5: 5729

46. Barkan A, Small I (2014) Pentatricopeptide repeat proteins in plants. *Annu Rev Plant Biol* 65: 415 – 442
47. Herbert CJ, Golik P, Bonnefoy N (2013) Yeast PPR proteins, watchdogs of mitochondrial gene expression. *RNA Biol* 10: 1477 – 1494
48. Steinmetz LM, Scharfe C, Deutschbauer AM, Mokranjac D, Herman ZS, Jones T, Chu AM, Giaever G, Prokisch H, Oefner PJ, *et al* (2002) Systematic screen for human disease genes in yeast. *Nat Genet* 31: 400 – 404
49. Moreno JI, Buie KS, Price RE, Piva MA (2009) Ccm1p/Ygr150cp, a pentatricopeptide repeat protein, is essential to remove the fourth intron of both COB and COX1 pre-mRNAs in *Saccharomyces cerevisiae*. *Curr Genet* 55: 475 – 484
50. Puchta O, Lubas M, Lipinski KA, Piatkowski J, Malecki M, Golik P (2010) DMR1 (CCM1/YGR150C) of *Saccharomyces cerevisiae* encodes an RNA-binding protein from the pentatricopeptide repeat family required for the maintenance of the mitochondrial 15S ribosomal RNA. *Genetics* 184: 959 – 973
51. Moreno JI, Patlolla B, Belton KR, Jenkins BC, Radchenkova PV, Piva MA (2012) Two independent activities define Ccm1p as a moonlighting protein in *Saccharomyces cerevisiae*. *Biosci Rep* 32: 549 – 557
52. Ting CT, Tsaur SC, Wu ML, Wu CI (1998) A rapidly evolving homeobox at the site of a hybrid sterility gene. *Science* 282: 1501 – 1504
53. Piskur J, Smole S, Groth C, Petersen RF, Pedersen MB (1998) Structure and genetic stability of mitochondrial genomes vary among yeasts of the genus *Saccharomyces*. *Int J Syst Bacteriol* 48(Pt 3): 1015 – 1024
54. Solieri L (2010) Mitochondrial inheritance in budding yeasts: towards an integrated understanding. *Trends Microbiol* 18: 521 – 530
55. Chou JY, Leu JY (2015) The Red Queen in mitochondria: cyto-nuclear co-evolution, hybrid breakdown and human disease. *Front Genet* 6: 187
56. O'Toole N, Hattori M, Andres C, Iida K, Lurin C, Schmitz-Linneweber C, Sugita M, Small I (2008) On the expansion of the pentatricopeptide repeat gene family in plants. *Mol Biol Evol* 25: 1120 – 1128
57. Hayes ML, Mulligan RM (2011) Pentatricopeptide repeat proteins constrain genome evolution in chloroplasts. *Mol Biol Evol* 28: 2029 – 2039
58. Hayes ML, Giang K, Mulligan RM (2012) Molecular evolution of pentatricopeptide repeat genes reveals truncation in species lacking an editing target and structural domains under distinct selective pressures. *BMC Evol Biol* 12: 66
59. Geddy R, Brown GG (2007) Genes encoding pentatricopeptide repeat (PPR) proteins are not conserved in location in plant genomes and may be subject to diversifying selection. *BMC Genom* 8: 130
60. Foxe JP, Wright SI (2009) Signature of diversifying selection on members of the pentatricopeptide repeat protein family in *Arabidopsis lyrata*. *Genetics* 183: 663 – 672
61. Dahan J, Mireau H (2013) The Rf and Rf-like PPR in higher plants, a fast-evolving subclass of PPR genes. *RNA Biol* 10: 1469 – 1476
62. Hanson MR, Bentolila S (2004) Interactions of mitochondrial and nuclear genes that affect male gametophyte development. *Plant Cell* 16 (Suppl): S154 – S169
63. Chase CD (2007) Cytoplasmic male sterility: a window to the world of plant mitochondrial-nuclear interactions. *Trends Genet* 23: 81 – 90
64. Barr CM, Fishman L (2010) The nuclear component of a cytonuclear hybrid incompatibility in mimulus maps to a cluster of pentatricopeptide repeat genes. *Genetics* 184: 455 – 465
65. Rieseberg LH, Blackman BK (2010) Speciation genes in plants. *Ann Bot* 106: 439 – 455
66. Chen L, Liu YG (2014) Male sterility and fertility restoration in crops. *Annu Rev Plant Biol* 65: 579 – 606
67. Horn R, Gupta KJ, Colombo N (2014) Mitochondrion role in molecular basis of cytoplasmic male sterility. *Mitochondrion* 19: 198 – 205
68. Tuppen HAL, Blakely EL, Turnbull DM, Taylor RW (2010) Mitochondrial DNA mutations and human disease. *BBA-Bioenergetics* 1797: 113 – 128
69. Lightowlers RN, Taylor RW, Turnbull DM (2015) Mutations causing mitochondrial disease: what is new and what challenges remain? *Science* 349: 1494 – 1499
70. Brandon M, Baldi P, Wallace DC (2006) Mitochondrial mutations in cancer. *Oncogene* 25: 4647 – 4662
71. Manolio TA, Collins FS, Cox NJ, Goldstein DB, Hindorff LA, Hunter DJ, McCarthy MI, Ramos EM, Cardon LR, Chakravarti A, *et al* (2009) Finding the missing heritability of complex diseases. *Nature* 461: 747 – 753
72. Lee SH, Wray NR, Goddard ME, Visscher PM (2011) Estimating missing heritability for disease from genome-wide association studies. *Am J Hum Genet* 88: 294 – 305
73. Lin TK, Lin HY, Chen SD, Chuang YC, Chuang JH, Wang PW, Huang ST, Tiao MM, Chen JB, Liou CW (2012) The creation of cybrids harboring mitochondrial haplogroups in the Taiwanese population of ethnic Chinese background: an extensive *in vitro* tool for the study of mitochondrial genomic variations. *Oxid Med Cell Longev* 2012: 824275
74. Kenney MC, Chwa M, Atilano SR, Falatoonzadeh P, Ramirez C, Malik D, Tarek M, Caceres-del-Carpio J, Nesburn AB, Boyer DS, *et al* (2014) Inherited mitochondrial DNA variants can affect complement, inflammation and apoptosis pathways: insights into mitochondrial-nuclear interactions. *Hum Mol Genet* 23: 3537 – 3551
75. Latorre-Pellicer A, Moreno-Loshuertos R, Lechuga-Vieco AV, Sanchez-Cabo F, Torroja C, Acin-Perez R, Calvo E, Aix E, Gonzalez-Guerra A, Logan A, *et al* (2016) Mitochondrial and nuclear DNA matching shapes metabolism and healthy ageing. *Nature* 535: 561 – 565
76. Rackham O, Filipovska A (2012) The role of mammalian PPR domain proteins in the regulation of mitochondrial gene expression. *Biochim Biophys Acta* 1819: 1008 – 1016
77. Mercer TR, Neph S, Dinger ME, Crawford J, Smith MA, Shearwood AM, Haugen E, Bracken CP, Rackham O, Stamatoyannopoulos JA, *et al* (2011) The human mitochondrial transcriptome. *Cell* 146: 645 – 658
78. Rackham O, Mercer TR, Filipovska A (2012) The human mitochondrial transcriptome and the RNA-binding proteins that regulate its expression. *Wiley Interdiscip Rev RNA* 3: 675 – 695
79. Ghaemmaghami S, Huh WK, Bower K, Howson RW, Belle A, Dephoure N, O'Shea EK, Weissman JS (2003) Global analysis of protein expression in yeast. *Nature* 425: 737 – 741
80. Ito H, Fukuda Y, Murata K, Kimura A (1983) Transformation of intact yeast cells treated with alkali cations. *J Bacteriol* 153: 163 – 168
81. Guthrie C, Fink G (2004) *Guide to yeast genetics and molecular and cell biology*. San Diego: Elsevier Academic Press
82. Goldring ES, Grossman LI, Krupnick D, Cryer DR, Marmur J (1970) The petite mutation in yeast. Loss of mitochondrial deoxyribonucleic acid during induction of petites with ethidium bromide. *J Mol Biol* 52: 323 – 335
83. Lemaire C, Dujardin G (2008) Preparation of respiratory chain complexes from *Saccharomyces cerevisiae* wild-type and mutant mitochondria: activity measurement and subunit composition analysis. *Methods Mol Biol* 432: 65 – 81
84. Sambrook J, Russell DW (2001) *Molecular cloning*. New York: Cold Spring Harbor Laboratory Press

85. Rodeheffer MS, Boone BE, Bryan AC, Shadel GS (2001) Nam1p, a protein involved in RNA processing and translation, is coupled to transcription through an interaction with yeast mitochondrial RNA polymerase. *J Biol Chem* 276: 8616 – 8622
86. Amiott EA, Jaehning JA (2006) Mitochondrial transcription is regulated via an ATP "sensing" mechanism that couples RNA abundance to respiration. *Mol Cell* 22: 329 – 338
87. Ellis TP, Helfenbein KG, Tzagoloff A, Dieckmann CL (2004) Aep3p stabilizes the mitochondrial bicistronic mRNA encoding subunits 6 and 8 of the H^+-translocating ATP synthase of *Saccharomyces cerevisiae*. *J Biol Chem* 279: 15728 – 15733
88. Selth LA, Gilbert C, Svejstrup JQ (2009) RNA immunoprecipitation to determine RNA-protein associations *in vivo*. *Cold Spring Harb Protoc* 2009: pdb.prot5234
89. Kallberg M, Wang HP, Wang S, Peng J, Wang ZY, Lu H, Xu JB (2012) Template-based protein structure modeling using the RaptorX web server. *Nat Protoc* 7: 1511 – 1522
90. Ma JZ, Wang S, Zhao F, Xu JB (2013) Protein threading using context-specific alignment potential. *Bioinformatics* 29: 257 – 265
91. Peng J, Xu J (2011) RaptorX: exploiting structure information for protein alignment by statistical inference. *Proteins* 79(Suppl 10): 161 – 171
92. Peng J, Xu J (2011) A multiple-template approach to protein threading. *Proteins* 79: 1930 – 1939
93. Yang Z (2007) PAML 4: phylogenetic analysis by maximum likelihood. *Mol Biol Evol* 24: 1586 – 1591
94. D'Andrea LD, Regan L (2003) TPR proteins: the versatile helix. *Trends Biochem Sci* 28: 655 – 662
95. Maris C, Dominguez C, Allain FH (2005) The RNA recognition motif, a plastic RNA-binding platform to regulate post-transcriptional gene expression. *FEBS J* 272: 2118 – 2131
96. Graack HR, Wittmann-Liebold B (1998) Mitochondrial ribosomal proteins (MRPs) of yeast. *Biochem J* 329(Pt 3): 433 – 448
97. Quenault T, Lithgow T, Traven A (2011) PUF proteins: repression, activation and mRNA localization. *Trends Cell Biol* 21: 104 – 112
98. Kehrein K, Schilling R, Moller-Hergt BV, Wurm CA, Jakobs S, Lamkemeyer T, Langer T, Ott M (2015) Organization of mitochondrial gene expression in two distinct ribosome-containing assemblies. *Cell Rep* 10: 843 – 853